ACS APPLIED MATERIALS & INTERFACES

Research Article

www.acsami.org

Advanced Anticorrosion Coating Materials Derived from Sunflower Oil with Bifunctional Properties

Thiruparasakthi Balakrishnan, Sadagopan Sathiyanarayanan, and Sundar Mayavan*

Corrosion and Material Protection Division, CSIR-Central Electrochemical Research Institute, Karaikudi 630 006, Tamil Nadu, India

Supporting Information

ABSTRACT: High-performance barrier films preventing permeation of moisture, aggressive chloride ions, and corrosive acids are important for many industries ranging from food to aviation. In the current study, pristine sunflower oil was used to form uniform adherent films on iron (Fe) via a simple single-step thermal treatment (without involving any initiator/mediator/catalyst). Oxidation of oil on heating results in a highly conjugated (oxidized) crystalline lamellar network with interlayer separation of 0.445 nm on Fe. The electrochemical corrosion tests proved that the coating exhibits superior anticorrosion performance with high coating resistance (>10^9 ohm cm^2) and low capacitance values (<10^{-10} F cm^{-2}) as compared to bare Fe, graphene, and conducting polymer based coatings in 1 M hydrochloric acid solutions. The electrochemical analyses reveal that the oil coatings developed in this study provided a two-fold protection of passivation from the oxide layer and barrier from polymeric films. It is clearly observed that there is no change in structure, morphology, or electrochemical properties even after a prolonged exposure time of 80 days. This work indicates the prospect of developing highly inert, environmentally green, nontoxic, and micrometer level passivating barrier coatings from more sustainable and renewable sources, which can be of interest for numerous applications.

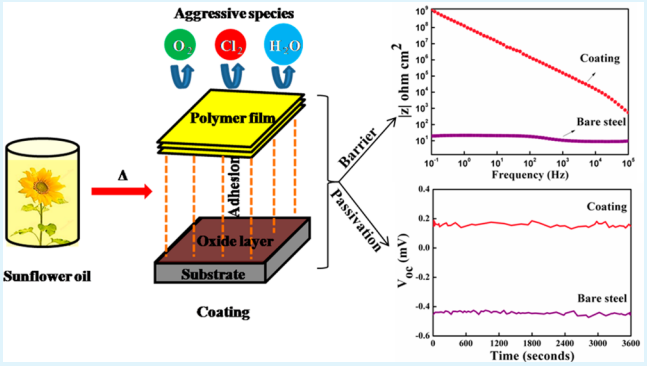

KEYWORDS: *sunflower oil, autoxidation, passivation, barrier, bifunctional property*

INTRODUCTION

The electrochemical degradation of metals on exposure to environmental conditions during their applications is termed corrosion.[1] However, corrosion can be controlled by transforming the metal into a cathode of an electrochemical cell as in the case of cathodic protection.[2] Another effective way is to transform it into a passive zone by applying anodic current as in the case of anodic protection.[3] A passive zone is characterized by the formation of oxides of the metal, which can effectively isolate the surface of the substrate from the electrolyte. Similarly, chromating based on hexavalent chromium oxide has been used for at least 60 years to form a corrosion-inhibiting passive layer over metals.[4] However, restrictions on the use of heavy metals and chromates in coating due to their toxic and carcinogenic nature paved the way toward the development of intrinsically conducting polymers (ICPs). ICPs represent a promising alternative to anodic passivation and chromating for the protection of metals, complementing or even replacing the application of external anodic currents.[5] ICPs, such as polypyrrole (PPy) and polyaniline (PANI), have an inherent oxidizing capability that induces a passive state of steels. However, the lack of well-defined structures, solubility in organic solvents, and poor mechanical properties are major issues associated with practical applications of PANI. It is still a highly challengeable task among researchers to have an ecofriendly, cost-effective, and high-performance polymeric coating with bifunctional properties that has the inherent capability to passivate the metal surface (as in case of ICPs) and simultaneously exhibit excellent barrier properties for metallic surfaces. Corrosion over mild steel can be inhibited or controlled by introducing stable protective polymeric coatings from renewable sources that prevents permeation of moisture, aggressive chloride ions, and corrosive acids. The disadvantages found in ICPs have been overcome by inhibitors/coatings derived from natural products. In this work, we demonstrate a facile strategy toward the development of bifunctional (both passivation and barrier properties) coatings from more sustainable renewable sources representing a promising alternative to coatings based on ICP, chromating, and anodic protection.

Among various renewable sources, vegetable oils (VO) are considered to be a nontoxic, nondepletable, domestically abundant, nonvolatile and biodegradable resource.[6] Polar molecules present in the oils can be absorbed on metal surfaces and form the corresponding metal oxides, which will enhance the stability of passivation and promote adhesion.[7]

Received: June 29, 2015
Accepted: August 21, 2015
Published: August 21, 2015

DOI: 10.1021/acsami.5b05789
ACS Appl. Mater. Interfaces 2015, 7, 19781−19788

Coatings based on VO date back to the days of cave paintings. The primary use of VO in coating is as a drying oil. Natural VOs are triacylglycerols of fatty acids with high degrees of unsaturated sites. Due to their unsaturation, they have the ability to form hydroperoxides, epoxies, hydroxyls or esters, etc., which can polymerize via cross-linking under certain conditions.[8] Until now, efforts have been made mostly to modify vegetable oils to produce blended coating material with improved physical properties. Lu and Larock[9−12] prepared a variety of waterborne polyurethane (PU) dispersions from plant oil and studied their thermal, mechanical, and antibacterial properties. Kessler et al.[13] prepared biobased PU from vegetable oils. In all of these approaches, either an initiator/modifier or multistep procedure has been utilized for the conversion of VO into an inhibitor for corrosion control. To the best of our knowledge no work has been reported on the use of only VO to form an advanced anticorrosion coating with bifunctional properties.

The current work developed a new pathway for the use of vegetable oil (sunflower oil) for inhibition of corrosion of metals. This simple and facile route results in a new polymeric material that provides both the barrier and passivation property for aggressive environments. The efficiency of inhibition depends on the mechanical, structural, and chemical characteristics of the formed film. The as-formed polymeric film was characterized through Fourier transform infrared spectroscopy (FTIR), X-ray diffraction (XRD), nuclear magnetic spectroscopy (NMR), atomic force microscopy (AFM), Raman spectroscopy, scanning electron microscopy (SEM), transmission electron microscopy (TEM), and X-ray photoelectron spectroscopy (XPS). The anticorrosion properties have been evaluated by electrochemical impedance spectroscopy (EIS) and polarization (Tafel plot) data. The mechanical properties, such as abrasion, adhesion, and hardness, were analyzed with cross-cut, Taber abrasion, and Koning pendulum tests. The prepared coating shows much better anticorrosion properties than graphene- and PANI-based polymer coatings.

RESULTS AND DISCUSSION

Characterization of Oil Film Formed on Fe. Sunflower oil is primarily made of triglycerides (TG), the main constituent of all vegetable oils. ^{13}C NMR spectra of as-received sunflower oil shown in Figure S1 show the characteristics of TG with the presence of terminal CH_3, CH_2, and allylic carbons in the range of 13.99−34.00 ppm, glyceryl CH_2 and CH carbon atoms at 61.8 and 68.59 ppm, olefinic (=C—H) carbon atoms at 127.59−129.91 ppm, and carbonyl (C═O) carbon atoms of the triester functionality at 172.53−172.94 ppm.[14] Unlike a single straight-chain compound, it has three branches each terminating with fatty acids. These are highly reactive molecules (at unsaturated sites) and have the inherent ability to form a solid, coherent, and adherent polymer film when spread on a steel surface. Scheme 1 illustrates the process for the facile synthesis of oil coating on mild steel surfaces (oil/Fe). After hand cleaning/polishing of the Fe surface, a drop of sunflower oil was applied on the Fe surface and annealed at 275 °C for 10 min. At this temperature, the triglycerides present in the oil undergo polymerization through oxidation. The reaction involves peroxide formation, decomposition of hydroperoxides, radical formation, and cross-linking.[8] Significant changes in the appearance and the physical and chemical states of the product with respect to the original oil are due to its oxidation. The thickness of the film formed over mild steel is 1.6 μm and is measured with AFM as given in Figure S2.

Figure 1 shows the FTIR spectra of sunflower oil (a) and the coating derived from it (b). The characteristic peaks of

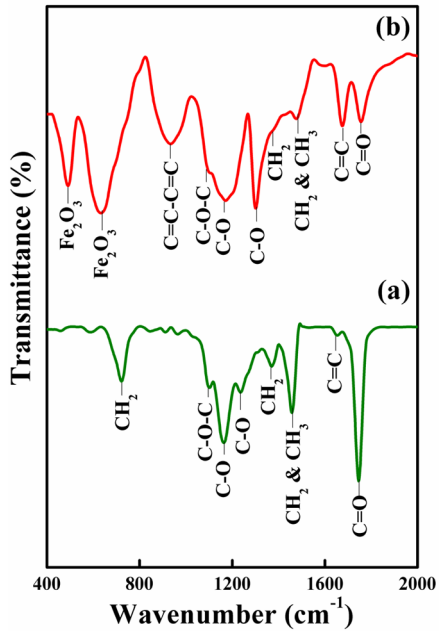

Figure 1. FTIR spectrum of (a) sunflower oil and (b) oil-baked film.

sunflower oil are obtained at 723 cm^{-1} (CH_2 rocking), 1165 and 1237 cm^{-1} (C—O ester group), 1372 and 1471 cm^{-1} (CH_2 and CH_3 bending), 1654 cm^{-1} (C═C stretching), and 1748 cm^{-1} (ester carbonyl group of triglycerides).[15] However, in the case of the as-formed film, there are metal oxide (Fe_2O_3) peaks at 478 and 628 cm^{-1} and a peak at 933 cm^{-1} due to the conjugation (−C═C—C═C).[16] The shifts in peaks from 1237 to 1298 cm^{-1} and from 1654 to 1674 cm^{-1} may be attributed to formed carboxylic groups (acids or its derivatives through cross-linking) and conjugation due to the shift of double bonds. The increase in intensity of C—O at 1298 cm^{-1} confirmed the highly oxidized state of resultant polymeric material, which means the formed film is highly oxidized. Thus, FTIR provides a clear picture about the higher degree of oxidation, the existence of conjugated double bonds, and the formed metal oxide layer due to the interaction between hydroperoxides and the metallic surface in the polymeric material.

The Raman spectrum was done to understand the oxidation degree of fatty acid (sunflower) on heating and is shown in Figure 2. The interval between 1000 and 1900 cm^{-1} is particularly important as it contains signals that are prone to being affected by the autoxidation of the fatty acid.[17] The peak at 1112 cm^{-1} reflects the combined effect of olefinic (CH) and aliphatic (CH_2 and CH_3) groups. Similarly, peaks at 1322 and

Scheme 1. Preparation of Highly Crystalline Film on Fe by Drop Casting and Heating the Sunflower Oil

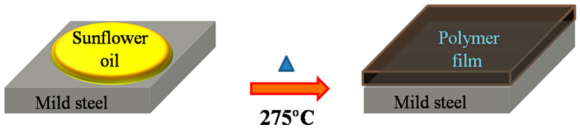

DOI: 10.1021/acsami.5b05789
ACS Appl. Mater. Interfaces 2015, 7, 19781−19788

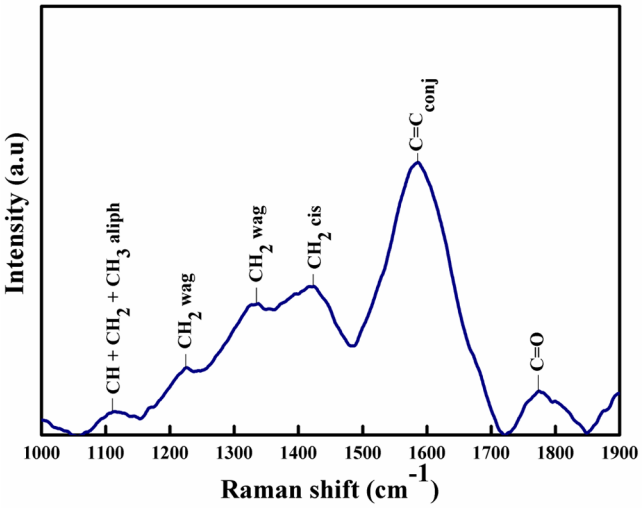

Figure 2. Raman spectroscopy of polymeric film obtained from sunflower oil.

1420 cm^{-1} are due to wagging and scissoring modes of CH_2 vibration. The isolated −C═C—C—C═C− (nonconjugated) double bond of the pure fatty acid exhibits a characteristic peak at around 1659 cm^{-1},[18] but the as-prepared film shows a high-intensity peak at 1598 cm^{-1}. This peak has not been reported widely in spectroscopic studies of the oxidation process of oil, and Machado et al.[18] assigned it to the out-of-phase (C═C) mode of the conjugated hydroperoxide groups. The formation of hydroperoxides indicates possible reaction between abstracted hydrogen and molecular oxygen (via peroxide route), reflecting the rearrangement from nonconjugated to highly conjugated fatty acids upon oxidation.[6] The peak at 1779 cm^{-1} is assigned to formed carboxylic groups upon oxidation of the oil.

XPS was done to analyze the chemical composition of oil-baked film. The XPS Survey spectrum shown in Figure S3 clearly indicates the presence of only carbon and oxygen. Figure 3a shows the high-resolution carbon C 1s spectra in which several chemical environments of carbon can be distinguished. The observed peaks correspond to C═O or C—OR (major component; 292.4 eV), methyl carbon (283.2 eV), C—O—C (286.5 eV), O—C═O (289.7 eV), and CO_2—R (294.9 eV), where R represents hydrogen or an alkyl substituent.[19] The peak at 296.3 eV is not widely explained and may be due to the oxygen (electronegative group) on both sides of the carbon atoms during cross-linking. Similarly, the high-resolution O 1s oxygen peak as shown in Figure 3b can be fitted at 530.5 eV (minor peak) and 539.4 eV (major peak), which corresponds to C═O and C—OR, respectively.[19] XPS and Raman data indicate the formation of a highly oxidized film as a result of the oxidation of oil, which introduces polarity into the polymer. These oxygen molecules are responsible for the inhibition property and adhesion existing between polymer and metal substrate through hydrogen bonding.

SEM was used to probe the morphologies of the as-prepared oil film. Figure S4 shows the smooth morphology of the coating surface without any nanostructures. Mechanically fractured cross-section images shown in Figure 4a,b clearly indicate the existence of lamellar-like layered structures. EDX spectra shown in Figure S5 and Table S1 confirm the presence of carbon and oxygen species. The observed layering of the crystallites provides evidence of the structure of a triglyceride (TG) crystal network.[19,20] The as-formed layered structures were broken (via sonication) to understand the fundamental structural units in the prepared film. TEM was used to image

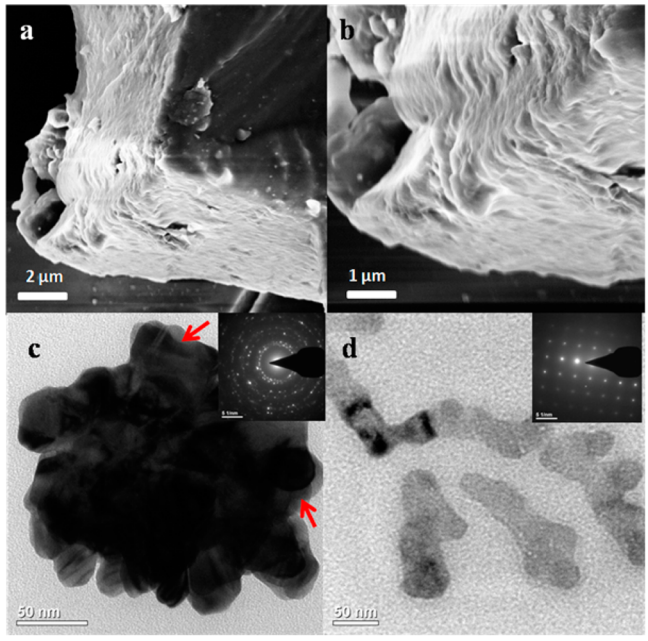

Figure 4. (a, b) FE-SEM and (c, d) TEM images of oil-baked film.

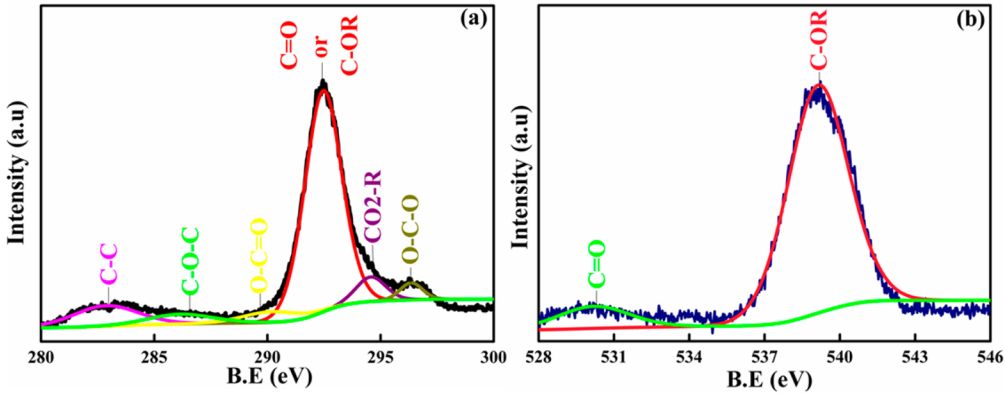

Figure 3. (a) C 1s and (b) O 1s high-resolution XPS spectra of oil-baked film.

DOI: 10.1021/acsami.5b05789
ACS Appl. Mater. Interfaces 2015, 7, 19781−19788

the broken network structure in the hope that information about the basic building blocks of the layered crystals could be obtained. For TEM, the as-prepared sample is probe sonicated in ethanol for about 3 h (very hard to disintegrate) and drop cast as a film. The TEM micrograph clearly indicates the coexistence of nonspherical polygon-like associates (Figure 4c) and nanofibrils (Figure 4d) with average widths of about 150 and 30−40 nm, respectively. Many isolated polygon-like associations were evident, and a representative one is shown in Figure 4c. The associations may be formed due to strong $\pi-\pi$ stacking between nanofibril segments.[20−22] Polygon-like associations show well-defined planar layered structures (marked by arrows in Figure 4c). SAED patterns (insets of Figure 4c,d) of polygon-like aggregates and nanofibrils indicate the polycrystalline and single-crystal nature, respectively, demonstrating the well-crystallized structure of the as-prepared film.

It is well established that TG in oil can adopt several crystalline arrangements (known as polymorphism). TG molecules can arrange themselves due to intermolecular interactions within a crystal lattice in a number of different ways of lateral packing of the fatty acid chains and of longitudinal stacking of molecules in lamellar structures. This lamellar or platelet-like structure of triglyceride molecules was assigned to be the more stable crystalline beta polymorph.[23] The packing arrangement of ethylene groups within the long fatty acid chains can be described using a subcell concept.

XRD is widely used to identify the crystalline subcell (interchain distance) characterizing the polymorphic forms. In Figure 5, the peaks at 44.56°, 64.96°, and 82.26° are ascribed to

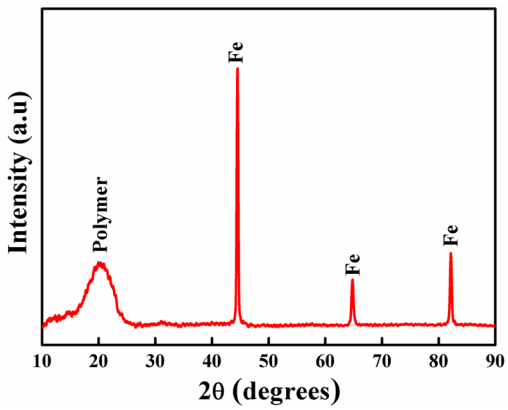

Figure 5. XRD pattern of sunflower oil coating on Fe.

the BCC structure of the Fe substrate. A single crystallite peak at 19.94° is close to the beta form with a subcell lamellar spacing of 0.445 nm.[22,23] The beta form is the densest polymorphic form having a triclinic chain packing, in which adjacent chains are in step ("parallel") and thus packed closely together. This clearly indicates that aggregation of nanofibril and layered nanostructures leads to the creation of layered mesoscale structure as observed in SEM.

Bifunctional Properties. To evaluate barrier properties, we have immersed oil/Fe samples in 1 M HCl. In this work HCl was selected as it has chloride ion aggressiveness coupled with an acidic nature. Digital photo images of oil/Fe specimens were takend after immersion for a period of 80 days (Figure 6a) at room temperature in air atmosphere. Despite the much smaller thickness of 1.6 μm (than conventional coating), the oil-baked film shows no trace of corrosion, delamination, or loss of adhesion even after 80 days of immersion in 1 M HCl aqueous solutions. On the other hand, it is noted that the surface of bare Fe is severely damaged (Figure 6b), and many corrosion products and pores can be seen on the surface (within a few days) caused by interaction with the electrolyte. The optical images show that the electrolyte has little or no effect in the case of oil/Fe; as a result, no corrosion product or delamination is observed.

We have further investigated the oil/Fe substrates using SEM (Figure 6c,d). No cracks or defects are evident in the oil-coated Fe even after 80 days of immersion in HCl. FTIR (Figure 6e,f) was used to analyze any degradation of oil film on prolonged immersion in 1 M HCl. The as-prepared oil/Fe shows characteristic TG peaks at 933, 1173, 1298, 1482, 1674, and 1756 cm^{-1}, indicating the presence of oil coating on the Fe substrate. After prolonged immersion for 80 days, no appreciable change in the FTIR spectra of oil coating on Fe was evident. Hence, it is clear from both SEM and FTIR data that the oil film acts as an excellent barrier against penetration of corrosive 1 M HCl acid even after prolonged immersion.

Electrochemical Characterization. Electrochemical impedance spectroscopy (EIS) was used to evaluate the barrier properties of the film against aggressive chloride ion attack present in 1 M HCl solution. Bode and Nyquist are the basic representations of EIS to evaluate the electrochemical degradation of coatings. Bode plots corresponding to exposure times of 1 and 80 days as shown in Figure 7A proved that the coating is highly capacitive. The slope of the high-frequency data is an indication of the mechanism of coating degradation. A slope of −1 over the entire spectrum indicates capacitive behavior, whereas a slope of −1/2 is an indication of diffusion control leading to substrate corrosion. Figure 7B shows Nyquist plots of bare Fe and oil/Fe samples kept in HCl. The plot for bare Fe exhibits semicircular characteristics with low resistivity to the corrosive medium. The oil/Fe sample corresponding to exposure times of 1 and 80 days in 1 M HCl provides a clear indication about capacitive behavior, consistent with an intact coating in the absence of defects.

Both the resistive and capacitive nature of the Fe and film is explained with the help of fitting the curves to appropriate equivalent circuits as shown in Scheme 2. R_s and R_p are solution ($\sim 10^2$ ohm/cm^2) and polarization resistance ($\sim 10^9$ ohm/cm^2), and C_{dl} and C_c are double-layer ($\sim 10^{-5}$ F/cm^2) and coating capacitance ($\sim 10^{-10}$ F/cm^2). Low-frequency impedance data allow assessment of total system resistance, in addition to providing information about the interaction of electrolyte (1 M HCl) at the metal−coating interface. The value of individual components of equivalent circuits corresponding to coating before and after immersion indicates practically there is no change in the impedance values. This indicates the process that initiates coating failure, which is characterized by decreasing impedance, simply does not occur during the 80 day exposure period. The reason for this can be related to outstanding barrier properties exhibited by the oil coating system. The coating exhibits capacitive behavior (with coating capacitance equivalent to $C_c = 1.359 \times 10^{-10}$ F) during the entire 80 day immersion period, which shows that there is no uptake of water from corrosive media. From EIS data, it was found that the corrosion resistance of oil/Fe was 8 orders of magnitude higher than that of uncoated Fe. For comparison, the commercially purchased refined soybean and corn oils were coated over the steel substrate with the same experimental condition. The FTIR

DOI: 10.1021/acsami.5b05789
ACS Appl. Mater. Interfaces 2015, 7, 19781−19788

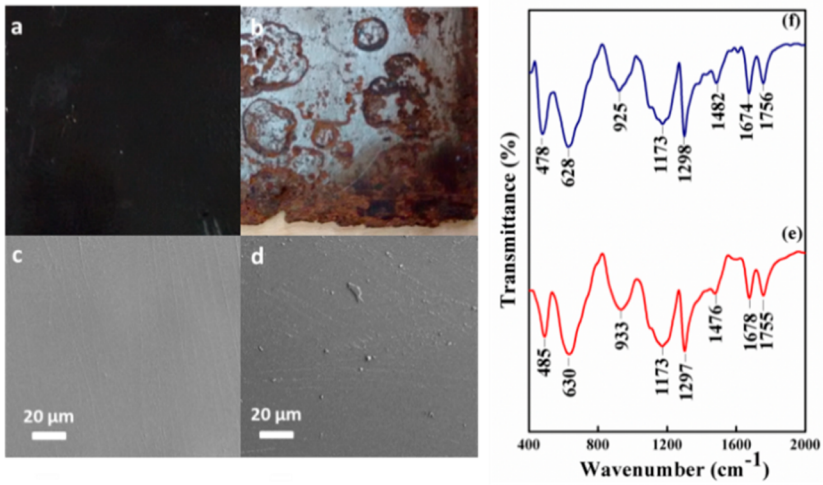

Figure 6. Optical image of (a) oil/Fe after 80 days of immersion in 1 M HCl and (b) bare steel in 1 M HCl after 5 days of immersion; SEM images of oil-annealed film on Fe (c) before immersion and (d) after 80 days of immersion in 1 M HCl; FTIR spectra of oil/Fe (e) before immersion and (f) after 80 days of immersion in 1 M HCl.

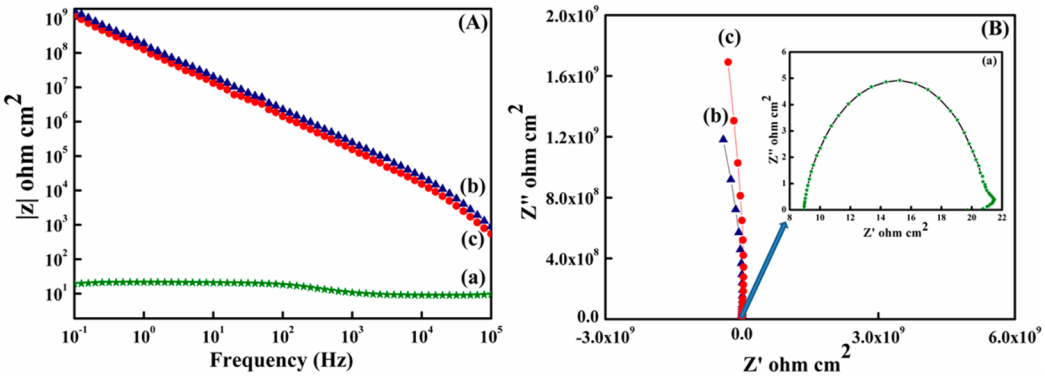

Figure 7. (A) Bode and (B) Nyquist plots for oil/Fe in 1 M HCl (a), bare Fe on day 1, (b) oil/Fe on day 1, and (c) oil/Fe on day 80.

Scheme 2. Equivalent Circuit Fitted to Bode/Nyquist Plot (a) Bare Mild Steel and (b) Oil/Fe Coating

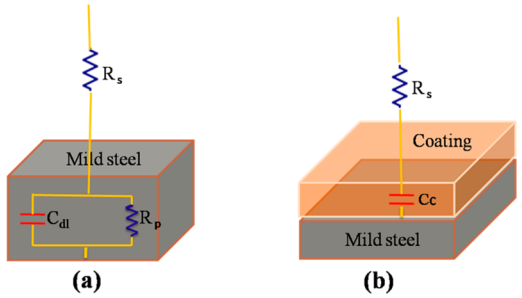

spectra of as-purchased oils and XRD of coatings derived from them proved that they are similar in characteristics with sunflower oil (Figure S6a,b). The impedance analysis of these oil coatings in 1 M HCl solution over 7 days of immersion shows similar behavior as observed in the case of sunflower oil coating (Figure S7).

In addition, the stability of the as-prepared sunflower oil coating was studied in 3.5% NaCl solution. The film shows no trace of corrosion, delamination, or loss of adhesion even after 7 days. Bode plots corresponding to exposure times of 1 and 7 days are shown in Figure S8, and the results show the coating is highly resistive (~10^9 ohm). We have tested the stability of coating using a salt spray test conducted as per ASTM B117 procedure. Rusting over the surface was observed for the bare steel and oil-coated samples after 6 and 60 h, respectively. As shown in Figure S9, the rust started to spread on the steel surface after 90 h, and 5% (in area) deterioration was observed after 120 h.

To compare the barrier properties of oil/Fe with graphene- and polymer-based coatings, we performed a comparative experiment with polystyrenesulfonate-coated Fe (PSS-Fe) and PSS functionalized reduced graphene oxide (r-GO) coated Fe samples. The coating resistance for PSS-Fe and r-GO/Fe is approximately 6 orders of magnitude lower than that of oil/Fe shown in Figure S10. Moreover, peeling off was evident in r-GO-coated film within a few days of immersion, indicating poor adhesion of r-GO-based films to metal surface. The results show that oil-baked film exhibits excellent barrier properties relative to polymer- and graphene-based coatings.

Polarization studies were performed, and a Tafel plot for bare Fe immersed in 1 M HCl for 60 min is shown in Figure 8a. In 1 M HCl solution (at acidic pH), the corrosion potential of bare Fe is located in the active region (−0.459 V) with a high current density of 0.0014 A/cm^2, but the highly resistive nature of the as-prepared oil coating (10^9 ohm/cm^2) does not allow us to polarize the interface, and we could only observe current (with distorted signals) in the pico-ampere range (10^{-12} A/cm^2) in the passive zone (between 0 and 0.5 V). To check the

DOI: 10.1021/acsami.5b05789
ACS Appl. Mater. Interfaces 2015, 7, 19781−19788

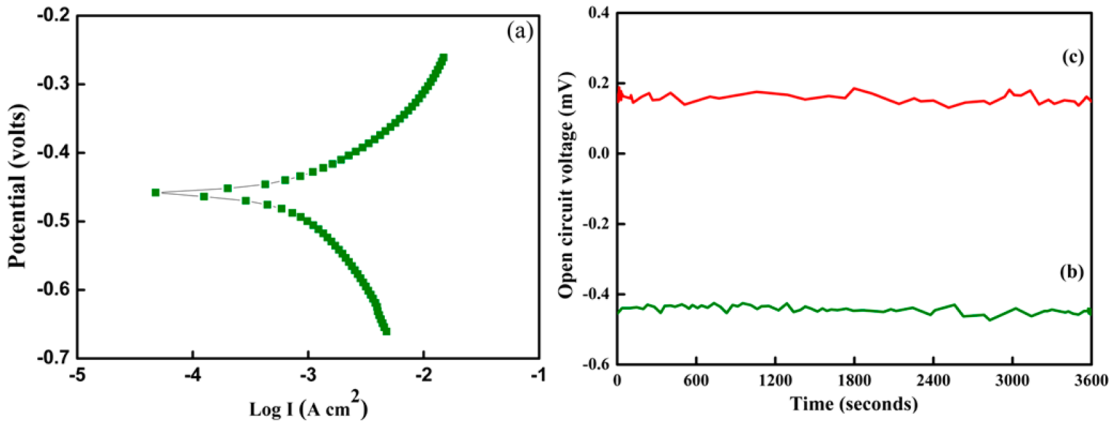

Figure 8. (a) Tafel plot of mild steel and OCP of (b) mild steel and (c) Fe/oil coating.

Table 1. Comparison of Mechanical and Electrochemical Properties of Coatings Obtained from Different Oils

		mechanical properties			electrochemical properties
sample	coating	aberration index (ASTM D4060)	adhesion (ASTM D3359)	hardness (*S*) (ASTM D4366)	impedance (ohm/cm^2)
1	sunflower oil	0.00105	5B	141.0	~10^9 and capacitive
2	soybean oil	0.00115	5B	142.1	~10^9 and capacitive
3	corn oil	0.00111	5B	141.1	~10^9 and capacitive

reproducibility, we conducted the experiment five times with five different samples, and similar trends were observed in all cases.

The corrosion passivation of the oil/Fe coating was tested in 1 M HCl solution by open circuit potential (OCP) measurement. OCP of samples shows that the oil/Fe sample is nobler than the bare Fe. The corrosion potential of oil/Fe is about +165 mV (Figure 8c). In contrast, the OCP of the bare Fe is around −445 mV (Figure 8b). For the oil/Fe sample the potential was shifted to noble direction in comparison with bare steel (ennobling). The observed ennobling is an indication of passivation. This shows that the as-prepared oil coating is able to passivate the iron surface in 1 M HCl. In the passive state, the corrosion rate of Fe becomes much lower as evidenced by current in the pico-ampere range in polarization data. The coatings obtained from soybean and corn oils also exhibit similar ennobling in 1 M HCl solutions with OCP values between +100 and 200 mV.

The oil coatings were scratch removed from the Fe substrate for characterizing the surface. SEM investigation revealed that there was an oxide layer (composed mainly by Fe_2O_3) present on the surface as shown in Figure S11. This confirms the formation of a passive layer on Fe, and this effect/behavior is similar to that of coatings based on ICPs. However, the coating resistance of the as-prepared oil coating is at least 2 orders of magnitude higher than observed with conducting polymer-based coatings, PANI-based polymer coatings,[24] and graphene-based coatings in 1 M HCl solution.

Mechanical Properties. The mechanical properties of coatings derived from sunflower, soybean, and corn oils were studied, and the results were compared with American Society for Testing and Materials (ASTM) standards. For realizing excellent barrier property, good adhesion between coating and substrate is essential. The adhesion of polymeric films over substrate was evaluated qualitatively by using a cross-cut method. For this, the coating surfaces are made into square lattices with the help of a cross-cutter. Pressure-sensitive Scotch tape was applied over it and then removed. The obtained results satisfied ASTM D3359 scale 5B, which implies there is no detachment of square lattices from the substrate surface and the edges are completely smooth as shown in Figure S12. These are characteristic of highly adherent coating systems. This indicates the film is highly adherent to metal surfaces. To understand the aberration of the coating, the coating surface is abraded using the rotary rubbing action of two wheels with a 500 g load. The weight of the samples before and after the test was measured and the weight loss calculated. It is observed that there is no damage of coatings over steel even after 1000 cycles (Figure S13) with less weight loss (1−2.5 mg). The abrasive resistance is expressed in terms of wear index (ASTM D4060) as follows.

$$I = \text{weight loss} \times \text{load}/\text{no. of cycles} \quad (1)$$

The calculated index values of coatings derived from the oils are in close to one another. The Koning pendulum experiment was done to understand the coating hardness. In this experiment, a pendulum resting on the coating surface is set into oscillation. The time for the amplitude of the swing to decrease from 6° to 3° was determined in seconds and is the measure of hardness of the coating. The observations made prove all coatings have above 140 s, which accounts for hard coatings. It is observed that all coatings are mechanically hard, highly adhesive, aberration resistant, and anticorrosive to the aggressive environment, and the measured values are indistinguishable from one another as shown in Table 1.

MECHANISM OF PROTECTION

The possible corrosion protection mechanism of baked film results from barrier protection and surface passivation. To explain the observed barrier properties of oil-baked film, we compared the permeation behavior of defect-free graphitic membranes. In graphene oxide, the width of capillaries varies from 0.7 to 1.3 nm.[25] Upon reduction, either chemically or thermally, interlayer separation decreases to 0.36 nm, which is close to the interlayer separation in graphite due to collapsing of capillaries. Hence, it is difficult for water and other molecules

DOI: 10.1021/acsami.5b05789
ACS Appl. Mater. Interfaces 2015, 7, 19781−19788

to permeate through graphene sheets, and molecules can diffuse only through structural defects.[25] In our case oil is heated at 275 °C and it forms highly ordered layered crystalline structures as evidenced by XRD, SEM, and TEM. The XRD peak at 19.94° (Figure 5) indicates the formation of the most dense crystal lamellar network (beta form) or, in other words, the highest degree of ordering or crystallization (lamellar morphology) with interchain separation of 0.445 nm on Fe (Scheme 3). The higher ordering and 0.445 nm interlayer spacing for as-prepared film ensure no scope for permeation of chloride ions and water molecules. Furthermore, the shift in potential to the noble region (Figure 8c) indicates that this coating is capable of passivating the steel surface (Scheme 3). Without passivation such a huge shift (around 600 mV) to positive potential is not possible. FTIR and SEM image confirm the formation of a passive oxide layer. The presence of highly conjugated and highly oxidized (Raman, XPS, and FTIR data) fatty acids may oxidize the metal surface to form a passive oxide layer as in the case of ICP. The presence of a large amount of polar groups (as evidenced by XPS data) ensures better adhesion between oil film and the metal substrate via secondary bonds or hydrogen bonds.[2] Hence, our coating provides both barrier protection (impermeable to chloride ions and water molecule) and surface passivation through a simple coating technique and hence the name "bi-functional".

Scheme 3. Anticorrosion Mechanism of Oil Coating on Steel Surface

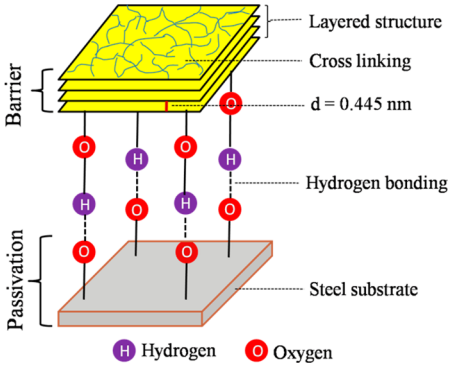

To the best of our knowledge this is the first work toward generating a high-performance barrier film with passivation behavior using vegetable oil by simple heating. The coating has the advantages of low cost, good mechanical properties, biocompatibility, and adhesion to metallic surfaces. Moreover, this coating formulation is more advantageous: the formulation of the coating is free from binder, solvents, additives, and any other supporting resin, which are essential for an efficient coating. Also, this ecofriendly and environmentally friendly green coating is a great alternative to synthetic conducting polymers.

CONCLUSION

In conclusion, for the first time oil-baked films with good mechanical properties are prepared by a simple approach and exhibit exceptional barrier and passivation properties with respect to aggressive hydrochloric acid, with no detectable corrosion even after 80 days of immersion. This would meet the stringent industry requirement for barrier coatings. The demonstrated films can be considered as flexible thin crystalline linings, which can be easily produced on metals on an industrial scale. Taking into account that the coating is produced from renewable sources, this work opens a venue for many applications requiring a barrier against moisture and acids for use in chemical and corrosion protection.

EXPERIMENTAL SECTION

Preparation of Oil-Baked Film on Mild Steel Substrate. The samples of mild steel with size of 4 × 4 cm^2 (coupons) were pickled in a dilute HCl acid and rinsed with deionized water to ensure a rust-free surface. The coupons were then surface polished using a rough abrasive paper of 320 grit followed by smooth abrasive paper of 600 and 1000 grit, degreased with acetone, and dried. These coupons were stored in a desiccator prior to coating. Fifty microliters of refined sunflower, soybean, or corn oil (commercially purchased) was drop cast on polished mild steel substrate and heated at 275 °C for 10 min in a furnace. Because sunflower oil has a higher content of unsaturated fatty acids, it is a thermodynamically unstable oil and undergoes oxidation upon heating and forms a polymer film on Fe.

Characterization. X-ray diffraction (XRD) patterns were measured using a Bruker D8 Advance X-ray diffractometer. FTIR spectra were recorded using a Nicolet 380 FTIR instrument having an ATR attachment (Thermo USA). Raman spectra were recorded using a high-resolution Renishaw Raman microscope employing a He−Ne laser of 1 mW at 514 nm. X-ray photoelectron spectroscopy (XPS) measurement was performed with a Sigma probe X-ray photoelectron spectrometer (Thermo VG Scientific) with Al Kα X-ray radiation as the X-ray source for excitation. The surface morphology was studied using a field emission scanning electron microscope (FE-SEM) (Carl Zeiss Supra 55VP/41/46) with an accelerating voltage of 15 kV using a SE detector. Energy-dispersive X-ray (EDX) analysis was performed with an EDAX detector installed on the SEM. A Philips-Tecnai F20 field-emission transmission electron microscopy (FE-TEM) apparatus operated at 200 kV was also used to observe the morphology of oil-baked film. The samples for TEM were prepared by placing a drop of the aqueous dispersion of oil-baked film on carbon-coated copper grids followed by drying. The hardness of the film was tested by using an Elcometer 3034−Pendulum hardness tester with Koning pendulum particularly used for hard coatings. Aberration of the samples was done by using a Taber Abraser model 503 with 500 g loadings. Adhesion test was performed using a cross-cutter, model Erichsen 295/II. Salt spray analysis was carried out with a salt spray test chamber, model Ascott S120T.

Electrochemical Measurements. EIS measurements were carried out on a PAR STAT 2273 Impedance analyzer (Princeton Applied Research) using a conventional three-electrode cell with a platinum counter electrode and a silver/silver chloride reference electrode. For Tafel polarization, the potential of the working electrode was scanned from −0.2 to +0.2 V versus open circuit potential (OCP) at the scan rate of 1 mV/s. From the anodic and cathodic polarization curves, the Tafel regions were identified and extrapolated to corrosion potential (E_{corr}) to get the corrosion current (I_{corr}) by using the auto-Tafel fit feature of Corrview software.

ASSOCIATED CONTENT

Supporting Information

The Supporting Information is available free of charge on the ACS Publications website at DOI: 10.1021/acsami.5b05789.

C 1s NMR spectrum of sunflower oil, AFM image for thickness measurement, XPS survey spectrum of coating, SEM images with EDX (top and bottom views), EIS spectra for impedance analysis, digital images of coatings subjected to salt spray test, and adhesion test (PDF)

AUTHOR INFORMATION

Corresponding Author

*(S.M.) Phone:91-4565-241453. E-mail:sundarmayavan@cecri.res.in.

DOI: 10.1021/acsami.5b05789
ACS Appl. Mater. Interfaces 2015, 7, 19781−19788

Author Contributions

The manuscript was written through contributions of all authors. All authors have given approval to the final version of the manuscript.

Notes

The authors declare no competing financial interest.

■ ACKNOWLEDGMENTS

This work was supported by DST-SERB Young Scientist Start-Up Research Grant (GAP 11/14) and CSIR project on "Intelligent Coatings (Intel Coat − CSC 0114)". We thank Dr. Syed Azim (Chief Scientist,Corrosion Materials Protection Division, CSIR-CECRI) and S. Subramanian (Project Fellow, Corrosion Materials Protection Division, CSIR-CECRI) for valuable discussion on abrasion, adhesion, hardness, and salt spray tests. We also thank CSIR-CECRI Central Instrumentation Facility for analytical support and Dr. S. Radhakrishnan, Er. A. Rathishkumar, Er. J. Kennedy, and Er. V. Prabhu for NMR, TEM, XPS, and FE-SEM analyses.

■ REFERENCES

(1) Jensen, H.; Sorensen, G. Ion Bombardment of Nano-Particle Coatings. *Surf. Coat. Technol.* **1996**, *84*, 500−505.
(2) Sørensen, P. A.; Kiil, S.; Dam-Johansen, K.; Weinell, C. E. Anticorrosive Coatings: A Review. *J. Coat. Technol. Res.* **2009**, *6*, 135−176.
(3) Perez, N. *Electrochemistry and Corrosion Science*; Springer Science & Business Media: Dordrecht, The Netherlands, 2004.
(4) Tallman, D. E.; Spinks, G.; Dominis, A.; Wallace, G. G. Electroactive Conducting Polymers for Corrosion Control. *J. Solid State Electrochem.* **2002**, *6*, 73−84.
(5) Spinks, G. M.; Dominis, A. J.; Wallace, G. G.; Tallman, D. E. Electroactive Conducting Polymers for Corrosion Control. *J. Solid State Electrochem.* **2002**, *6*, 85−100.
(6) Lligadas, G.; Ronda, J. C.; Galià, M.; Cádiz, V. Renewable Polymeric Materials from Vegetable Oils: A Perspective. *Mater. Today* **2013**, *16*, 337−343.
(7) Powers, R. A.; Cessna, J. C. How Polar-Type Oils Inhibit Corrosion. *Ind. Eng. Chem.* **1959**, *51*, 891−892.
(8) Alam, M.; Akram, D.; Sharmin, E.; Zafar, F.; Ahmad, S. Vegetable Oil Based Eco-Friendly Coating Materials: A Review Article. *Arabian J. Chem.* **2014**, *7*, 469−479.
(9) Xia, Y.; Zhang, Z.; Kessler, M. R.; Brehm-Stecher, B.; Larock, R. C. Antibacterial Soybean-Oil-Based Cationic Polyurethane Coatings Prepared from Different Amino Polyols. *ChemSusChem* **2012**, *5*, 2221−2227.
(10) Lu, Y.; Larock, R. C. Aqueous Cationic Polyurethane Dispersions from Vegetable Oils. *ChemSusChem* **2010**, *3*, 329−333.
(11) Lu, Y.; Larock, R. C. Soybean-Oil-Based Waterborne Polyurethane Dispersions: Effects of Polyol Functionality and Hard Segment Content on Properties. *Biomacromolecules* **2008**, *9*, 3332−3340.
(12) Lu, Y.; Larock, R. C. New Hybrid Latexes from a Soybean Oil-Based Waterborne Polyurethane and Acrylics via Emulsion Polymerization. *Biomacromolecules* **2007**, *8*, 3108−3114.
(13) Zhang, C.; Madbouly, S. A.; Kessler, M. R. Biobased Polyurethanes Prepared from Different Vegetable Oils. *ACS Appl. Mater. Interfaces* **2015**, *7*, 1226−1233.
(14) Jie, M. S. F. L. .K.; Mustafa, J. High-Resolution Nuclear Magnetic Resonance Spectroscopy − Applications to Fatty Acids and Triacylglycerols. *Lipids* **1997**, *32*, 1019−1034.
(15) Vlachos, N.; Skopelitis, Y.; Psaroudaki, M.; Konstantinidou, V.; Chatzilazarou, A.; Tegou, E. Applications of Fourier Transform-Infrared Spectroscopy to Edible Oils. *Anal. Chim. Acta* **2006**, *573*−*574*, 459−465.
(16) Kadamne, J. V.; Jain, V. P.; Saleh, M.; Proctor, A. Measurement of Conjugated Linoleic Acid (CLA) in CLA-Rich Soy Oil by Attenuated Total Reflectance− Fourier Transform Infrared Spectroscopy (ATR− FTIR). *J. Agric. Food Chem.* **2009**, *57*, 10483−10488.
(17) Muik, B.; Lendl, B.; Molina-Díaz, A.; Ayora-Cañada, M. J. Direct Monitoring of Lipid Oxidation in Edible Oils by Fourier Transform Raman Spectroscopy. *Chem. Phys. Lipids* **2005**, *134*, 173−182.
(18) Machado, N. F. L.; de Carvalho, L. A. E. B.; Otero, J. C.; Marques, M. P. M. The Autooxidation Process in Linoleic Acid Screened by Raman Spectroscopy. *J. Raman Spectrosc.* **2012**, *43*, 1991−2000.
(19) O'Toole, L.; Short, R. D. An Investigation of the Mechanisms of Plasma Polymerisation of Allyl Alcohol. *J. Chem. Soc., Faraday Trans.* **1997**, *93*, 1141−1145.
(20) Maleky, F.; Smith, A. K.; Marangoni, A. Laminar Shear Effects on Crystalline Alignments and Nanostructure of a Triacylglycerol Crystal Network. *Cryst. Growth Des.* **2011**, *11*, 2335−2345.
(21) Truong, T.; Morgan, G. P.; Bansal, N.; Palmer, M.; Bhandari, B. Crystal Structures and Morphologies of Fractionated Milk Fat in Nanoemulsions. *Food Chem.* **2015**, *171*, 157−167.
(22) Marangoni, A. G.; Acevedo, N.; Maleky, F.; Co, E.; Peyronel, F.; Mazzanti, G.; Quinn, B.; Pink, D. Structure and Functionality of Edible Fats. *Soft Matter* **2012**, *8*, 1275−1300.
(23) Bunjes, H.; Steiniger, F.; Richter, W. Visualizing the Structure of Triglyceride Nanoparticles in Different Crystal Modifications. *Langmuir* **2007**, *23*, 4005−4011.
(24) Sathiyanarayanan, S.; Muthkrishnan, S.; Venkatachari, G. Corrosion Protection of Steel by Polyaniline Blended Coating. *Electrochim. Acta* **2006**, *51*, 6313−6319.
(25) Su, Y.; Kravets, V. G.; Wong, S. L.; Waters, J.; Geim, A. K.; Nair, R. R. Impermeable Barrier Films and Protective Coatings Based on Reduced Graphene Oxide. *Nat. Commun.* **2014**, *5*, 4843.

DOI: 10.1021/acsami.5b05789
ACS Appl. Mater. Interfaces 2015, 7, 19781−19788